Supplemental figures and figure legends

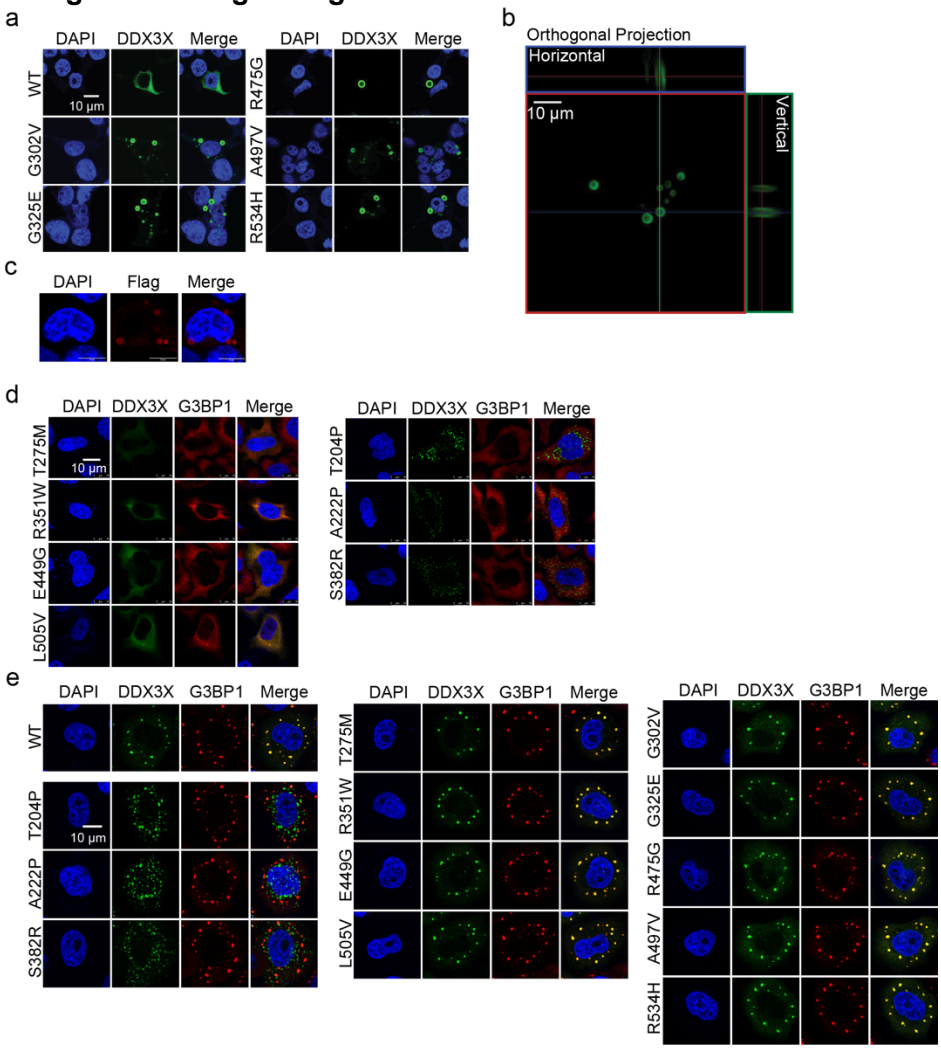

Supplemental Fig. 1: A subset of DDX3X disease mutants form unique hollow condensates in cells.

a, Representative images of cellular distributions of the mClover3-tagged DDX3X mutants in HEK293T cells. Scale bar, 10 µm. **b,** Orthogonal projections demonstrate that mClover3-tagged R475G forms puncta, enriched in the spherical shell but less intense in the (seemingly) hollow core. Scale bar, 10 µm. **c,** Representative images of Flag-G325E in HEK293T cells stained with an anti-Flag antibody. Scale bar, 8 µm. **d,** Representative images of the indicated mClvoer3-tagged WT DDX3X or DDX3X mutants and the mCherry-tagged stress granule marker G3BP1 in HeLa cells. Top, diffuse mutants. Bottom, speckle mutants. Scale bar, 10 µm. **e,** Representative images of indicated mClover3-tagged WT DDX3X or DDX3X mutants and the mCherry-tagged stress granule marker G3BP1 in HeLa cells upon arsenite treatment (500 µM, 1 hr). Scale bar, 10 µm. All imaging was performed in three biological replicates.

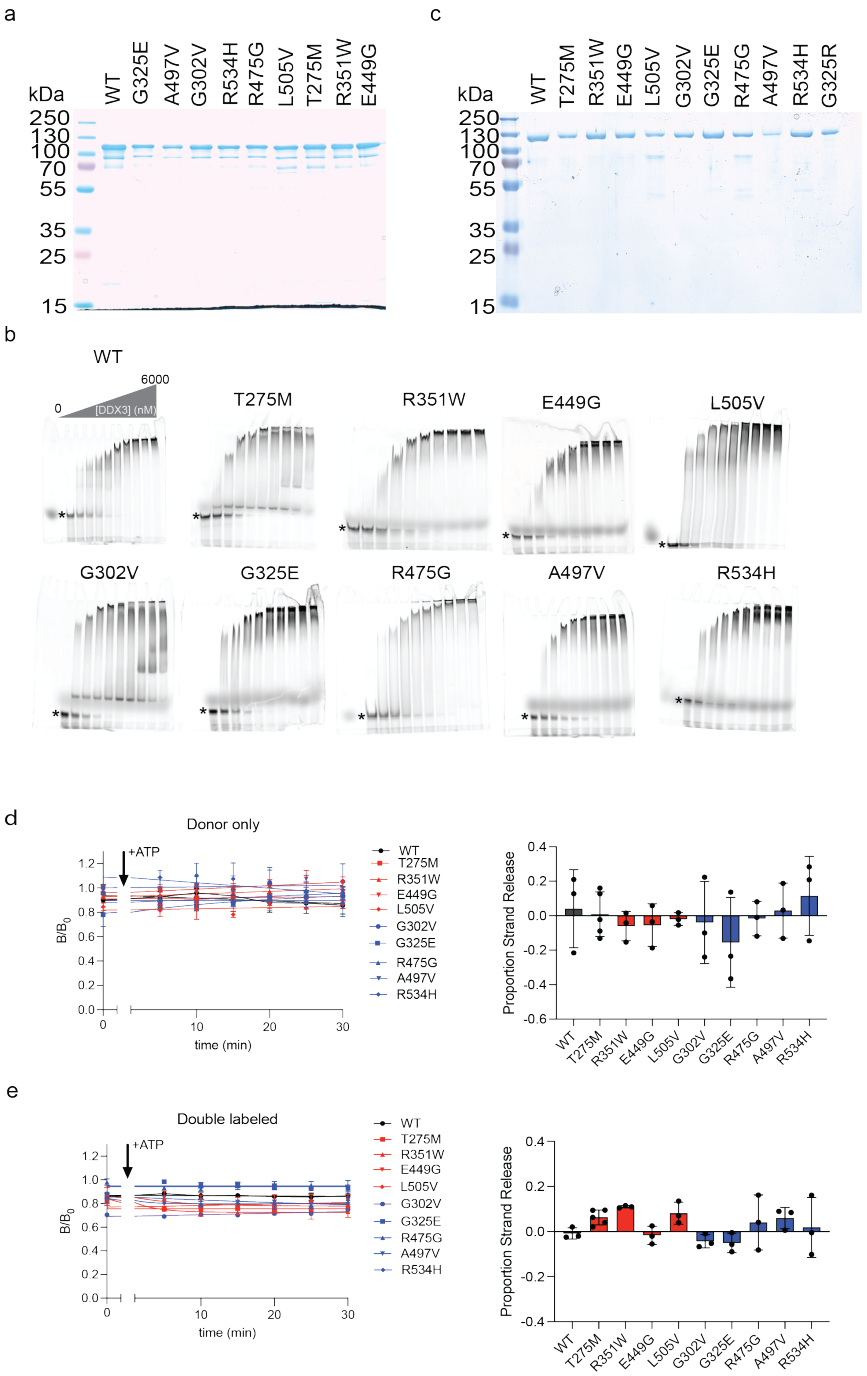

Supplemental Fig. 2: Hollow mutants are characterized by their decreased ATPase and strand release activities.

a, Coomassie-stained SDS-PAGE gel showing each purified mCherry-tagged construct. **b,** Representative EMSAs for each indicated construct. Fraction unwound was calculated for each construct by quantifying the disappearance of the unbound ssRNA (indicated by the *) at each concentration as described in methods. **c,** Coomassie-stained SDS-PAGE gel showing each purified MBP-tagged construct. **d,** Left, time courses tracing the B/B_0 (or fraction anisotropic) for long strand (donor only) RNA over time in the presence of 1 mM ATP and MBP-tagged WT DDX3X

or the indicated mutants, fit as described in Methods. Right, proportion strand release graphed for each protein. Values represent mean ± s.d., n = 3 independent replicates (n = 5 for T275M). **e,** Left, time courses tracing the B/B_0 (or fraction anisotropic) for duplex strand RNA (double labeled) over time in the presence of 1 mM ATP and MBP-tagged WT DDX3X or the indicated mutants, fit as described in Methods. Right, proportion strand release graphed for each protein. Values represent mean ± s.d., n = 3 independent replicates (n = 5 for T275M). Source data are provided as a Source Data file.

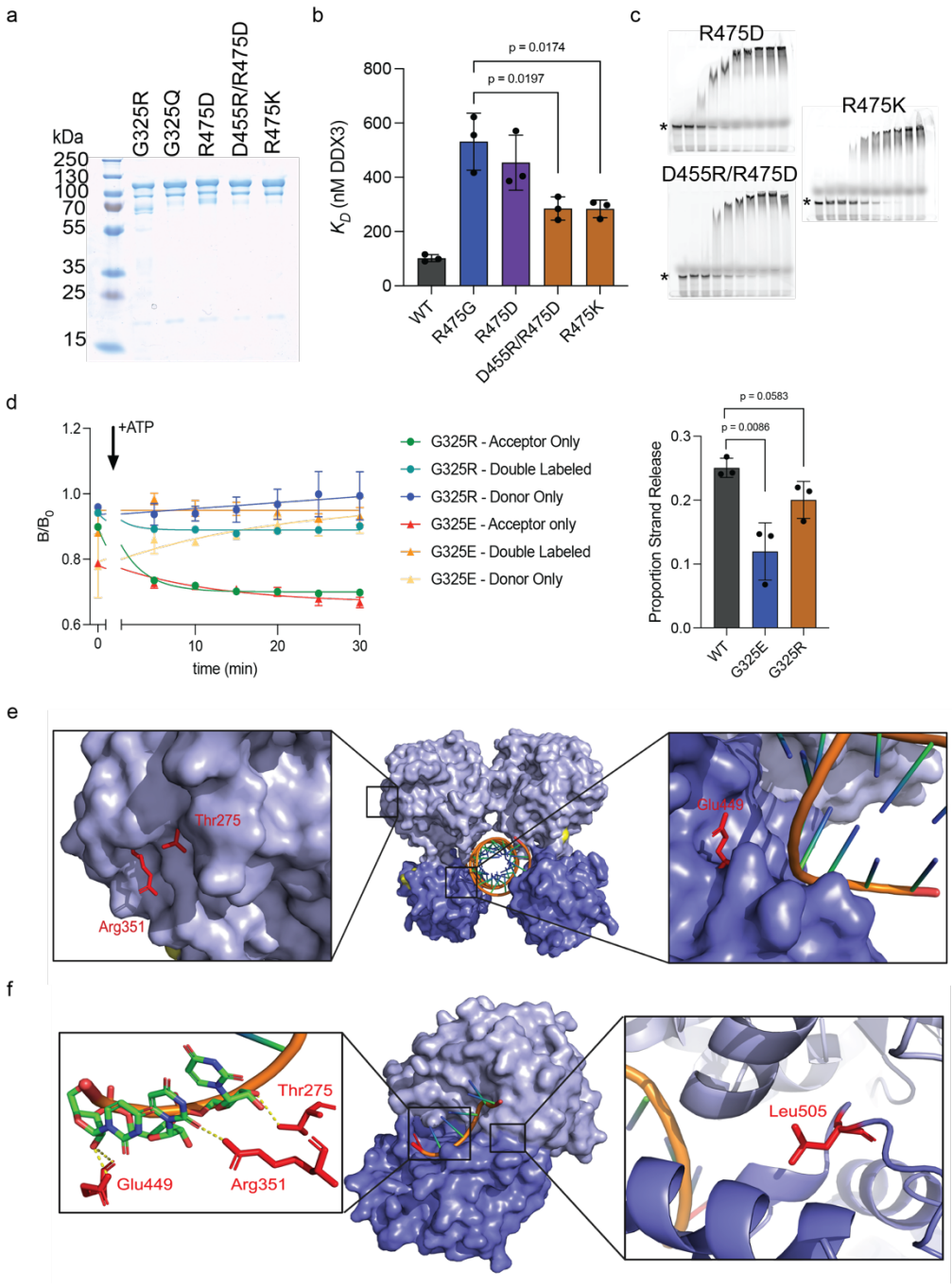

Supplemental Fig. 3: Mechanistic studies reveal how DDX3X mutants interfere with catalysis.

a, Coomassie-stained SDS-PAGE gel showing each purified mCherry-tagged rescue mutant construct. **b,** Summarized K_D values for the indicated construct, calculated via EMSA using mCherry-tagged protein. Values represent mean ± s.d., n = 3 independent experiments. Significance was calculated using a two-tailed t test. **c,** Representative EMSAs for each indicated construct. Fraction unwound was calculated for each construct by quantifying the disappearance of the unbound ssRNA (indicated by the *) at each concentration as described in methods. **d,** Left, time courses tracing the B/B_0 (or fraction anisotropic) for short strand, long strand, and duplex RNA over time in the presence of 1 mM ATP and the indicated MBP-tagged protein. Right, proportion strand release graphed for each protein. Values represent mean ± s.d., n = 3

independent replicates. Significance was calculated using a two-tailed t test. **e**, Pre-unwound structure of DDX3X expanded around Thr275 and Arg351 (left) and Glu449 (right). **f**, Post-unwound structure of Vasa expanded around Thr275, Arg351, Gly449 (left) and Leu505 (right) (numbered according to DDX3X homology). Dashed lines represent hydrogen bonds between each indicated residue and the RNA backbone. Source data are provided as a Source Data file.

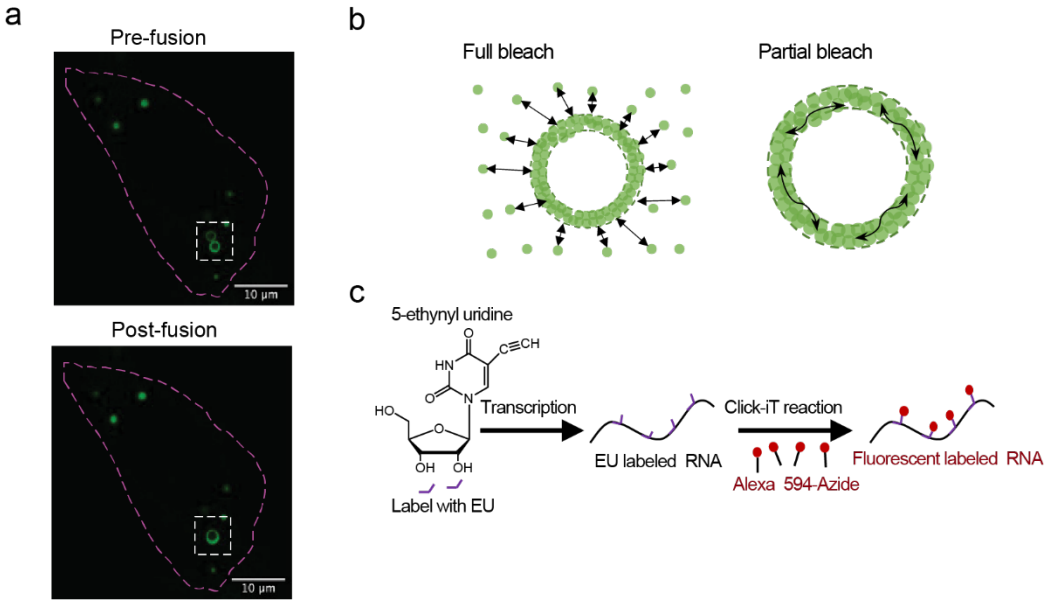

Supplemental Fig. 4: RNA-binding affinity differentiates the inter- and intramolecular dynamics of DDX3X hollow puncta. a, Representative still images of live-cell imaging showing the fusion of two hollow puncta of G325E-mClover3 in HeLa cells. Scale bar, 10 µm. **b,** Schematic of full bleach and partial bleach FRAP assays. Full bleach experiments were used to test for molecular exchange between the cytoplasm and hollow condensates (intermolecular). Partial bleach was used to test for the mobility of molecules within the hollow condensates (intramolecular). **c,** Schematic of the EU-labeling experiments. All imaging was performed in three biological replicates.

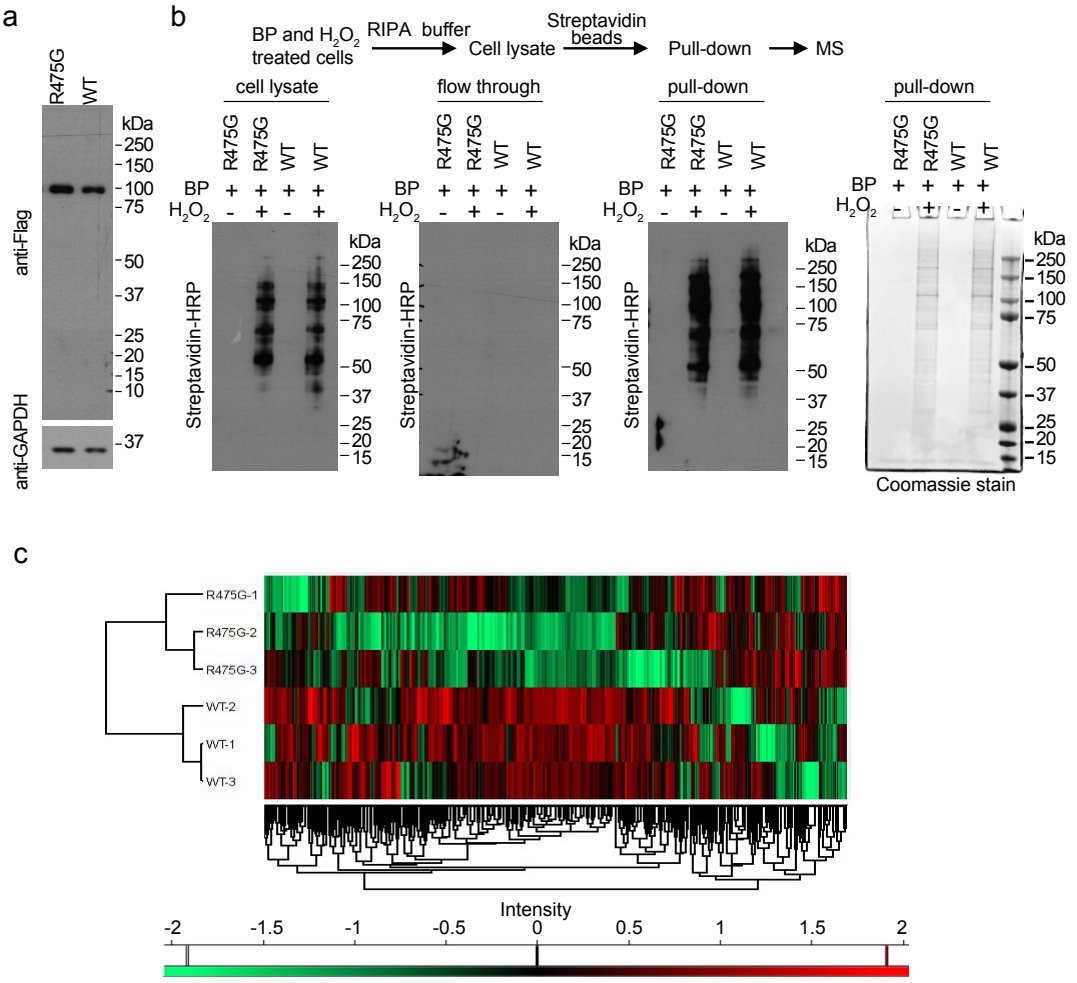

Supplemental Fig. 5: R475G hollow condensates enrich proteins in various signaling pathways and deplete translation machinery.

a, Western blots showing the comparable expression of APEX2-tagged WT and R475G DDX3X in HEK293T cells. **b,** Top panel: workflow of the APEX2-MS sample preparation. Bottom panel: western blots and Coomassie stain showing the number of labeled proteins in the cell lysates, flow through, and pull-down fractions of streptavidin pull-down. BP: biotin phenol. **c,** Unsupervised hierarchical cluster analyses of protein abundances from quantitative APEX2-MS analyses of WT and R475G biological triplicates.

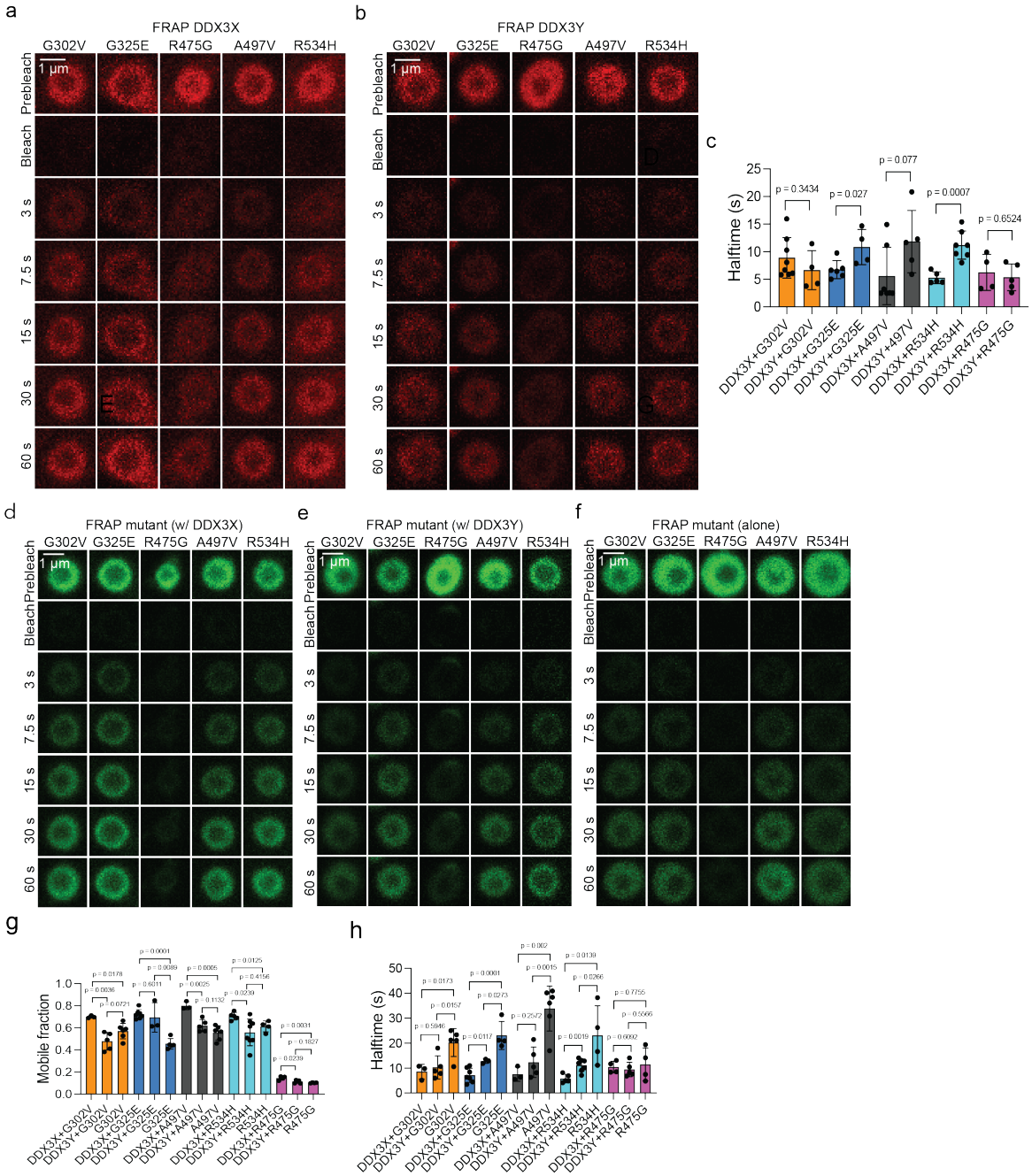

Supplemental Fig. 6: Mutant hollow condensates trap WT DDX3X and DDX3Y.
a, Time-lapsed images of photobleached mCherry-tagged WT DDX3X trapped in the cytoplasmic hollow condensates formed by mClover3-tagged DDX3X hollow mutants in HeLa cells from the cellular FRAP experiments. Scale bar, 1 µm. **b,** Time-lapsed images of photobleached mCherry-tagged WT DDX3Y trapped in the cytoplasmic hollow condensates formed by mClover3-tagged DDX3X hollow mutants from the cellular FRAP experiments. Scale bar, 1 µm. **c,** Comparison of FRAP recovery halftimes of DDX3X and DDX3Y trapped in the cytoplasmic hollow condensates formed by DDX3X mutants. Halftime was calculated as described in the Methods. Values

represent means ± s.d. w/ DDX3X: n = 8 for G302V, 5 for R534H, 6 for G325E, 4 for R475G, and 7 for A497V. w/ DDX3Y, n = 4 for G302V, 7 for R534H, 4 for G325E, 5 for R475G, and 5 for A497V (biologically independent samples). Significance was calculated using a two-tailed t-test. **d,** Time-lapsed images of photobleached mClover3-tagged mutant DDX3X in the cytoplasmic hollow co-condensates with mCherry-tagged WT DDX3X in HeLa cells from the cellular FRAP experiments. Scale bar, 1 μm. **e,** Time-lapsed images of photobleached mClover3-tagged mutant DDX3X in the cytoplasmic hollow co-condensates with mCherry-tagged DDX3Y in HeLa cells from the cellular FRAP experiments. Scale bar, 1 μm. **f,** Time-lapsed images of photobleached mClover3-tagged mutant DDX3X in the cytoplasmic hollow condensates when expressed alone in HeLa cells from the cellular FRAP experiments. Scale bar, 1 μm. **g,** Comparison of the FRAP mobile fractions of the indicated mClover3-tagged DDX3X mutant in cytoplasmic hollow condensates either alone, with mCherry-tagged WT DDX3X or mCherry-tagged WT DDX3Y. The mobile fraction was calculated as described in the Methods. Values represent means ± s.d. n = 5 for G325E, 4 for R475G, 6 for A497V, 6 for G302V, and 4 for R534H (biologically independent samples). Significance was calculated using a two-tailed t-test. **h,** Comparison of the FRAP recovery halftimes of the indicated mClover3-tagged DDX3X mutant in cytoplasmic hollow condensates either alone, with mCherry-tagged WT DDX3X or mCherry-tagged WT DDX3Y. Halftime was calculated as described in the Methods. Values represent means ± s.d. n = 5 for G325E, 4 for R475G, 6 for A497V, 6 for G302V, and 4 for R534H (biologically independent samples). Significance was calculated using a two-tailed t-test. Source data are provided as a Source Data file.